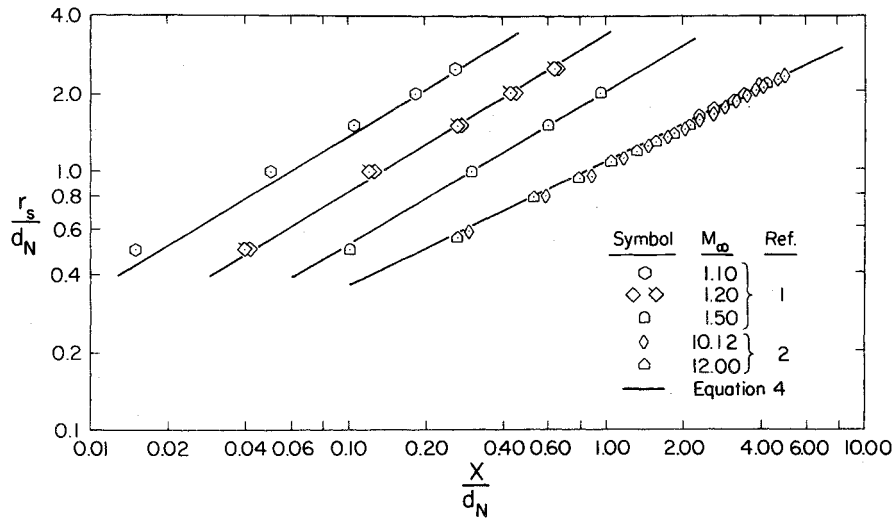

Fig. 2 Comparison of experimental bow shock profiles and results of present empirical correlation.

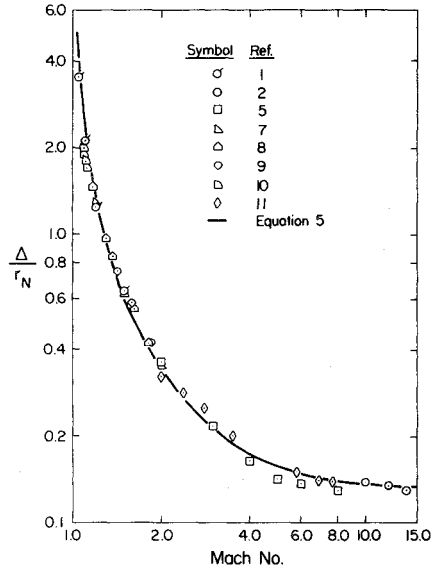

Fig. 3 Comparison of experimental shock detachment distance and existing empirical correlation as a function of freestream Mach number.

flowfield or to provide/verify the results of existing numerical approaches.

References

[1]Hsieh, T., "Hemisphere-Cylinder in Low Supersonic Flow," *AIAA Journal*, Vol. 13, Dec. 1975, pp. 1551-1552.

[2]Gregorek, G. M. and Korkan, K. D., "Hypersonic Blunt Body Similitude in a Perfect Gas," FDL-TDR-64-92, June 1964.

[3]Korkan, K. D., "Comments on 'Bow Shock Shape About a Spherical Nose,'" *AIAA Journal*, Vol. 4, Feb. 1966, pp. 381-382.

[4]Seiff, A. and Whiting, E. E., "A Correlation Study of the Bow Wave Profiles of Blunt Bodies," NASA TN D-1148, Feb. 1962.

[5]Baer, A. L., "Pressure Distributions ona Hemisphere Cylinder at Supersonic and Hypersonic Mach Numbers," AEDC-TN-61-96, Aug. 1961.

[6]Love, E. S., "A Re-examination of the Use of Simple Concepts for Predicting the Shape and Location of Detached Shock Waves," NACA TN-4170, Dec. 1957.

[7]Gilinskii, S. M. and Lebedev, M. G., "Investigation of a Flow at Low Supersonic Speeds—Past Plane and Axisymmetric Bodies with a Separated Shock Wave," Akademiia Nauk SSSR, *Izvestiia Mekhanika*, Jan.-Feb. 1965.

[8]Herberle, J. W., Wood, G. P., and Gooderum, P. B., "Data on Shape and Location of Detached Shock Waves on Cones and Spheres," NACA TN 2000, Jan. 1950.

[9]Holder, D. W. and Chinneck, A., "The Flow Past Elliptic-nosed Cylinders and Bodies of Revolution in Supersonic Air Streams," *The Aeronautical Quarterly*, Vol. IV, No. 2, Feb. 1954.

[10]Stlip, A., "Stromungsuntersuchungen an Kugeln mit transonischen und supersonischen Geschwindigkeiten in Luft und Frigen-Luftgemischen," Bericht Nr. 10/65, Ernst-Mach-Institut, Freiburg, Germany, 1965.

[11]Ambrosio, A. and Wortman, A., "Stagnation Point Shock Detachment Distance for Flow Around Spheres and Cylinders in Air," *Journal of the Aerospace Sciences*, Vol. 29, No. 7, July 1962.

Study of the Turbulent Near Wake of a Flat Plate

M.L. Agrawal,* P.K. Pande,† and Rajendra Prakash‡
University of Roorkee, Roorkee, India

Introduction and Analysis

ONE of the important aspects of fluid flow past submerged bodies is the study of flow characteristics at the trailing edge. While a number of such studies have been made for bodies of different shapes in laminar flow,[1-3] information for the case of turbulent flows is rather scanty. A number of investigators have studied the far wake of a submerged body and the results are well documented.[2,4-6] The studies available on the near wake are, however, limited.[6,8,10,14,15] For the case of flow past a flat plate at zero incidence, writing the momentum balance for a control volume as shown in Fig. 1, and combining it with Reichardt's momentum transfer law one gets Reichardt's fundamental equation for free turbulence[16]

$$\frac{\partial \overline{u^2}}{\partial x} - \beta \frac{\partial^2 \overline{u^2}}{\partial y^2} = 0 \tag{1}$$

in which u is the instantaneous velocity in the x-direction and β the momentum transfer length. Substituting

$$\bar{u} = u + u' \tag{2}$$

Received Nov. 30, 1976; revision received Feb. 25, 1977.
Index category: Jets, Wakes, and Viscid-Inviscid Flow Interactions.

*Reader, Mechanical Engineering, Govt. Engineering College, Bilaspur, M.P., India, presently working as Research Fellow.
†Professor, Department of Civil Engineering.
‡Professor, Department of Mechanical and Industrial Engineering.

in which $\bar{u}$ and u' are the time average and fluctuating components respectively of the velocity, and neglecting $\bar{u'}^2$ and $2\bar{u}u'$ as compared to $\bar{u}$,

$$\partial\bar{u}^2/\partial x - \beta\partial^2\bar{u}^2/\partial y^2 = 0 \tag{3}$$

with the boundary conditions

$$\bar{u}=u \text{ at } y=\pm\infty \text{ and } \bar{u}^2=u_e^2-g_o(y) \text{ at } x=0 \tag{4}$$

in which $g_o(y)$ is the distribution of $(\bar{u}_e^2-\bar{u}^2)$ at the trailing edge, $\bar{u}_e$ being the freestream velocity. Defining

$$\bar{x}=x/\theta_o,\ \bar{y}=y/\theta_o,\ u=\bar{u}/\bar{u}_e,\ K^2=\beta/\theta_o$$

$$E=(1-u^2) \text{ and } T=\int_o^{\bar{x}} K^2 d\bar{x} \tag{5}$$

in which θ_o is twice the momentum thickness of the boundary layer at the trailing edge, Eq. (3) can be written in the form

$$\partial E/\partial T=\partial^2 E/\partial\bar{y}^2 \tag{6}$$

with the boundary conditions

$$\bar{y}=\pm\infty,\ E=0,\ T=0,\ E=g_o(\bar{y}) \tag{7}$$

Equations (6) is similar to the equation of one-dimensional nonsteady heat conduction, for which solutions are available in terms of error functions. The solution E at various values of T was obtained using a step by step scheme for numerical integration. This gives the velocity u and velocity defect u_D at various values of x. The computations were made on an IBM 1620 digital computer.

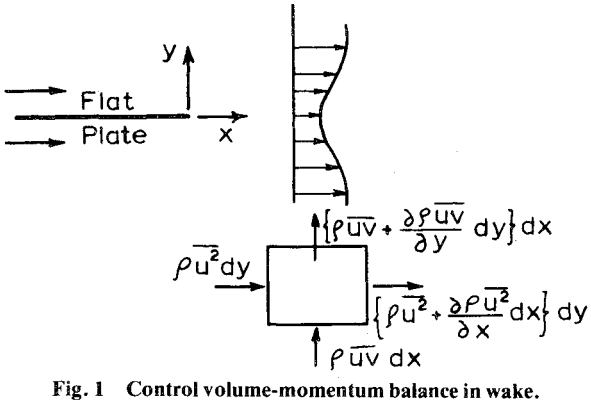

Fig. 1 Control volume-momentum balance in wake.

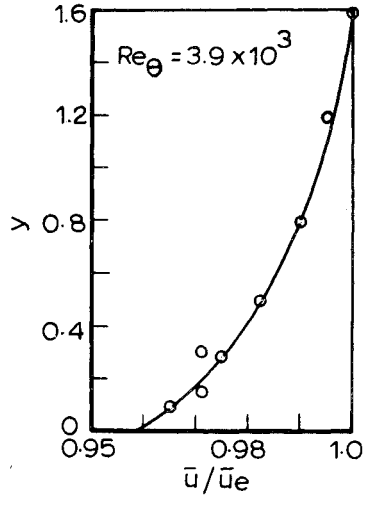

Fig. 2 Velocity distribution on plate.

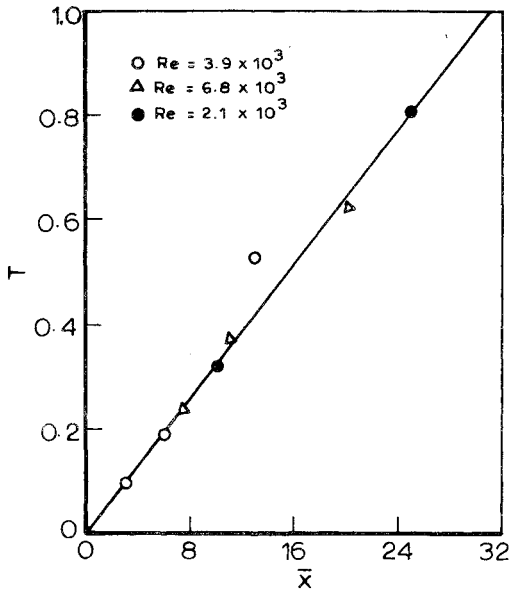

Fig. 3 Variation of T with $\bar{x}$.

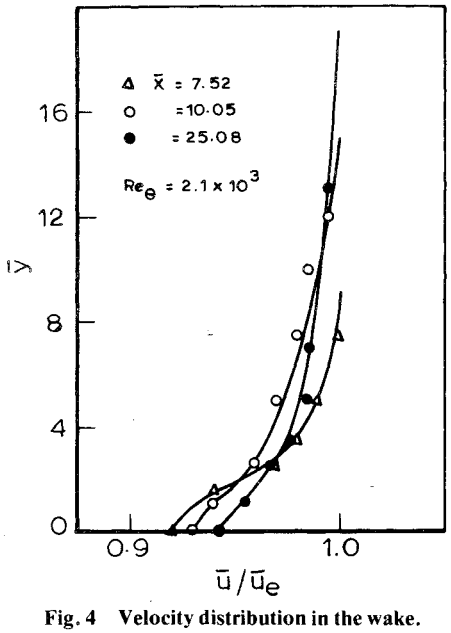

Fig. 4 Velocity distribution in the wake.

Experimental Program and Discussion of Results

The experiments were carried out in an open circuit wind tunnel having a test section 33.5 cm × 33.5 cm and 4.9 m long. A plate 33 cm. wide, 50 cm long and 0.15 cm thick was mounted in the tunnel along the midstream and measurements of mean velocities and turbulence intensities were made using a single-wire probe with a Flow-Corporation Model 900-C constant temperature hot wire anemometer.

The velocity distribution over the plate at a distance of 3 mm upstream of the trailing edge is shown in Fig. 2. The distribution is shown for one side of the plate only as the other side showed symmetrical profiles as expected. The variation of T with $\bar{x}$ is shown in Fig. 3. The points for various Reynolds number ($Re_\theta = u_e\theta_o/\nu$) fall on a single straight line, giving a value of $K^2 = 0.0325$ which compares favorably with Townsend's[5] value of $K^2 = 0.032$ for a circular cylinder. The velocity distribution and velocity defect at various axial distances downstream of the trailing edge are shown in Figs. 4 and 5 respectively. The figures also show the theoretical results i.e. solutions of Eq. (6). As can be seen, there is a fair agreement between the theoretical and experimental results

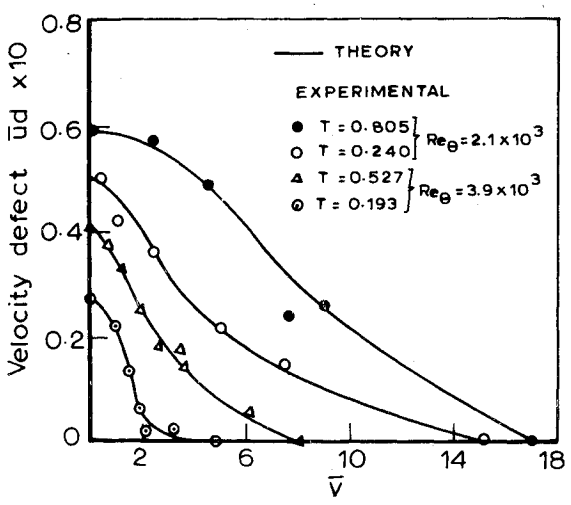

Fig. 5 Velocity defect distribution.

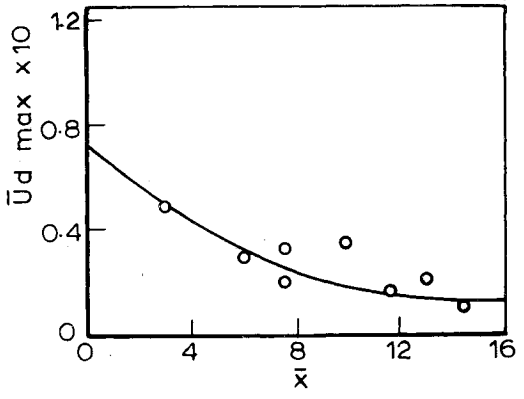

Fig. 6 Variation of max velocity defect with $\bar{x}$.

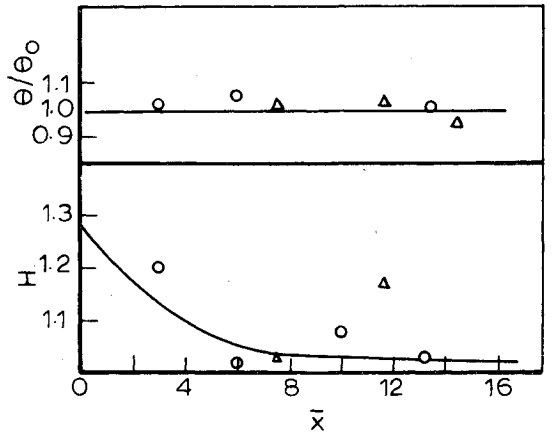

Fig. 7 Variation of H and θ/θ_o with $\bar{x}$.

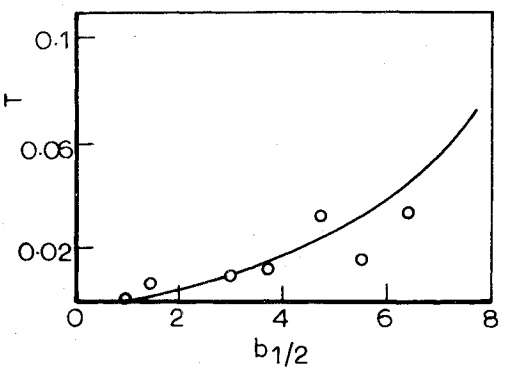

Fig. 8 Relation of T and half wake width $B_{1/2}$.

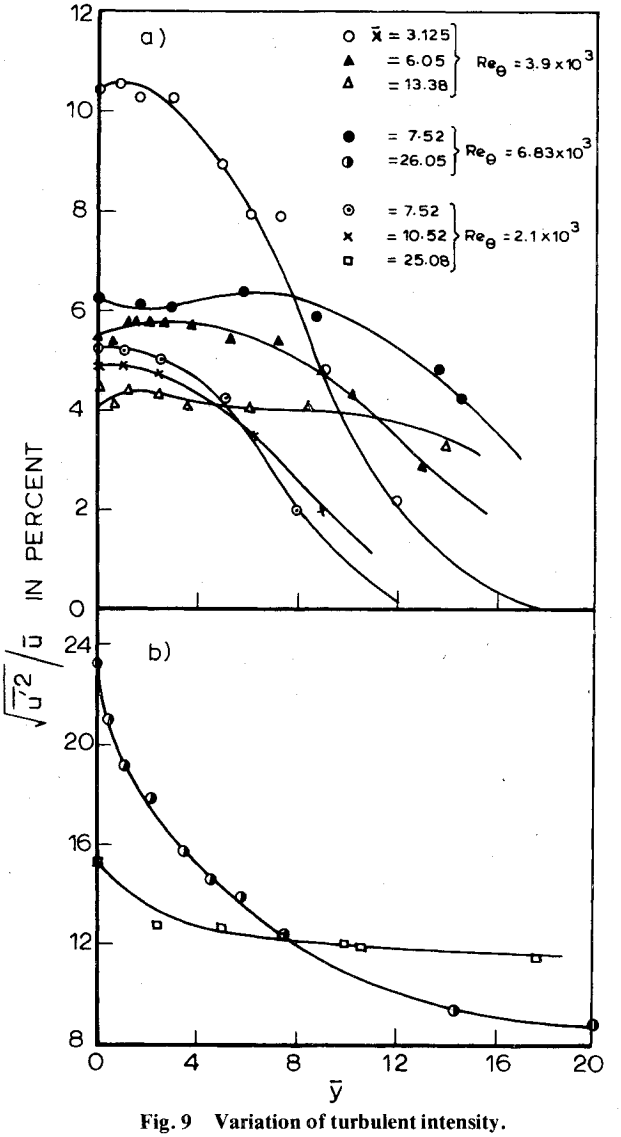

Fig. 9 Variation of turbulent intensity.

for various Reynolds numbers. The maximum velocity defect distribution is shown in Fig. 6. The results correspond to a value of the shape parameter $H_o = 1.283$ where H_o is defined as the ratio of the displacement thickness δ_o and momentum thickness θ_o at the trailing edge. Larger values of the maximum velocity defect have been reported by ElAssar and Page[8] and Chevray and Kovasznay[15] for higher values of H_o viz. 1.4 and 1.44 respectively.

The variation of momentum thickness ratio θ/θ_o and shape parameter H with axial distance $\bar{x}$ is shown in Fig. 7. While θ/θ_o remains constant at a value of 1.0, H is large in the beginning but very soon attains a constant value thereby justifying the assumption of constant pressure in the wake. Figure 8 shows the distribution of the half width of wake with T. The values are smaller compared to those reported by ElAssar and Page,[8] Cheveay and Kovasznay[15] and Toyoda and Hirayama.[14] Figure 9a shows the variation of turbulence intensity in the wake for values of $\bar{x}<20$ and follows a trend similar to those reported by Townsend[5] and Kovasznay.[15] For values of $\bar{x}>20$ however, the nature of the curve changes as shown in Fig. 9b. Chevray and Kovasnay[15] have classified the wake of a cylinder for $x/\theta_o > 30$ as the far-wake and in this region the turbulence intensity distribution is similar in nature to that shown by Fig. 9b. Similar results are reported by Toyoda and Hirayama[14] for $\bar{x}>31.3$. Thus the present study would indicate $\bar{x}=20$ as the limit at which the near wake

changes to the far wake. This however, needs further experimental verification.

Conclusion

The measured velocity distribution and velocity defect distribution in the near wake of a flat plate agree fairly well with the values obtained by solving Reichardt's fundamental equation for free turbulence. The momentum transfer coefficient K^2 has the same order of magnitude as obtained by Townsend[12] for circular cylinders. The turbulence intensity variation shows two distinct patterns, one for $\bar{x}=20$ may be the limit at which the near wake changes to the far wake. This however, needs more detailed experimental investigation. The effect of shape parameter H_o at the trailing edge also needs to be investigated further as it seems to have a definite bearing on the wake characteristics.

References

[1]Kiya, M. and Arie M., "An Analysis of Laminar Wake Behind a Symmetrical Two-Dimensional Body in a Uniform Shear Flow," *Bulletin of the JSME*, Vol. 16, Sept. 1973, pp. 1301-1313.

[2]Kiya, M. and Arie, M., "A Perturbation Analysis of the Laminar Far Wake Behind a Symmetrical Two-Dimensional Body in a Uniform Shear Flow," *Journal of Fluid Mechanics*, Vol. 61, Pt. 2, 1973, pp. 305-321.

[3]Talke, F.M. and Berger, S.A., "The Flat Plate Trailing Edge Problem," *Journal of Fluid Mechanics*, Vol. 40, 1970, p. 161.

[4]Schlichting, H., *Boundary Layer Theory*, McGraw Hill, New York, 1960.

[5]Townsend, A.A., *The Structure of Turbulent Shear Flow*, Cambridge University Press, London, 1956.

[6]Toyoda, K. and Hirayama, N., "Turbulent Near Wake of a Flat Plate, Part II," *Bulletin of JSME*, Vol. 18, June 1975, pp. 605-611.

[7]Torda, T.P., Ackermann, W.P., and Burnett, H.R., "Symmetrical Turbulent Mixing of Two Parallel Streams," *Journal of Applied Mechanics*, March 1953, p. 3.

[8]ElAssar, R.J. and Page, R.H., "Incompressible Turbulent Wake of a Flat Plate," *AIAA Journal*, Vol. 7, July 1969, pp. 1388-1389.

[9]Lee, S.C. and Harsha, P.T., "Use of turbulent kinetic energy in free mixing studies," *AIAA Journal*, Vol. 8, June 1970, pp. 1026-1032.

[10]Bradshaw, P., "Prediction of the Turbulent Near Wake of a Symmetrical Aerofoil," *AIAA Journal*, Vol. 8, Aug. 1970, pp. 1507-1508.

[11]Carmody, T., "Establishment of the Wake Behind a Disk," *Transactions of the ASME, Series D*, Vol. 86, 1964, p. 869.

[12]Harsha, P.T. and Lee, S.C., "Correlation Between Turbulent Shear Stress and Turbulent Kinetic Energy," *AIAA Journal*, Vol. 8, Aug. 1970, pp. 1508-1510.

[13]Auiler, J.E. and Lee, S.C., "The Theory of Two-Dimensional Turbulent Wakes," *AIAA Journal*, Vol. 8, Oct. 1970, pp. 1876-1878.

[14]Toyoda, K. and Hirayama, N., "Turbulent Near Wake of a Flat Plate, Part I, Incompressible Flow," *Bulletin of the JSME*, Vol. 17, June 1974, pp. 707-712.

[15]Chevray, R. and Kovasznay, L.S.G., "Turbulence Measurements in the Wake of a Thin Flat Plate," *AIAA Journal*, Vol. 7, 1969, pp. 1641-1643.

[16]Hinze, J.O., *Turbulence*, McGraw Hill, New York, 1959, p. 290.

Modal Synthesis for Combined Structural-Acoustic Systems

Joseph A. Wolf Jr.*
General Motors Research Laboratories, Warren, Mich.

Introduction

THE modal synthesis technique is widely used in structural modeling for dynamics. This method, its history and development are well described in a survey paper presented in 1971 by Hurty.[1] The purpose of this Note is to cast the dynamics of a combined structural-acoustic system in terms of a modal synthesis. This approach appears to be especially useful for determining the low-frequency free and forced interior acoustical properties of the passenger compartments of road and rail vehicles and aircraft wherein the acoustic wavelength is of the same order of magnitude as the dimensions of the structure. As with most such efforts, the goal of this work is to produce cost and time savings in the analysis task. For the examples discussed below, the procedure described herein results in a significant reduction in computer cost from that required for solution of the complete system, with little loss in accuracy.

Received Dec. 13, 1976.

Index categories: Structural Dynamic Analysis; Aircraft Noise, Aerodynamics (including Sonic Boom).

*Senior Research Engineer, Engineering Mechanics Department.

Analysis

Development of the finite element method has produced renewed interest in the structural-acoustic problem by making tractable the solution for arbitrary geometries.[2-8] As a starting point for the present development, we take the equations of motion of the coupled system in the form given by Everstine, et al.[9]

$$\begin{bmatrix} [M_{ss}] & [0] \\ [M_{fs}] & [M_{ff}] \end{bmatrix} \begin{Bmatrix} \{\ddot{u}\} \\ \{\ddot{p}\} \end{Bmatrix} + \begin{bmatrix} [K_{ss}] & [K_{sf}] \\ [0] & [K_{ff}] \end{bmatrix} \begin{Bmatrix} \{u\} \\ \{p\} \end{Bmatrix} = \begin{Bmatrix} \{F_s\} \\ \{0\} \end{Bmatrix} \tag{1}$$

where $\{u\}$ is the vector of n normal displacements for the compartment structure, $\{p\}$ is the vector of m nodal pressures for the enclosed fluid, $[M_{ss}]$ and $[K_{ss}]$ are the $n\times n$ structural mass and stiffness matrices, $[M_{ff}]$ and $[K_{ff}]$ are the $m\times m$ fluid mass and stiffness matrices, $[K_{sf}]=[A]$ and $[M_{fs}]=-(\rho c)^2\,[A]^T$, with $[A]$ a sparse $n\times m$ coupling matrix whose elements are found from the surface area A_{ij} for the boundary node corresponding to the structural displacement u_i and the associated fluid pressure at that node p_j. Also, ρc is the characteristic impedance of the fluid, and $\{F_s\}$ is the vector of external forces applied to the structure.

For brevity, in the remainder of this development, we will consider a free, harmonic solution of Eq. (1), such that $\{F_s\}=\{0\}$ and $\{\ddot{u}\}=-\omega^2\{u\}$, $\{\ddot{p}\}=-\omega^2\{p\}$. The extension to include forced motion can be carried out in the usual way. Furthermore, we will employ a transformation of coordinates, using the structural modes $[\phi_s]$ determined *in vacuo* and the rigid wall acoustic cavity modes $[\phi_f]$, such that

$$\{u\}=[\phi_s]\ \{\eta_s\} \tag{2a}$$

$$\{p\}=[\phi_f]\ \{\eta_f\} \tag{2b}$$

with $\{\eta_s\}$ and $\{\eta_f\}$ representing the appropriate modal coordinates.

Making these substitutions, and premultiplying all terms by

$$\begin{bmatrix} [\phi_s]^T & [0] \\ [0] & [\phi_f]^T \end{bmatrix}$$

gives the desired result

$$-\omega^2 \begin{bmatrix} \lceil M_s \rfloor & [0] \\ -(\rho c)^2[C]^T & \lceil M_f \rfloor \end{bmatrix} \begin{Bmatrix} \{\eta_s\} \\ \{\eta_f\} \end{Bmatrix} + \begin{bmatrix} \lceil K_s \rfloor & [C] \\ [0] & \lceil K_f \rfloor \end{bmatrix} \begin{Bmatrix} \{\eta_s\} \\ \{\eta_f\} \end{Bmatrix} = \{0\} \tag{3}$$

where $[C]=[\phi_s]^T\,[A]\,[\phi_f]$, the modal coupling matrix, and $\lceil M_s \rfloor=[\phi_s]^T\,[M_{ss}]\,[\phi_s]$, etc. Note that the elements of $[C]$ represent the product of the structural "ring" modes with